# Photoconductive Detection of Tetrahedrally Coordinated Hydrogen in ZnO

S. G. Koch, E. V. Lavrov,* and J. Weber
*Technische Universität Dresden, 01062 Dresden, Germany*

(Received 4 January 2012; published 20 April 2012)

In this Letter we apply an innovative experimental approach, which allows us to improve the sensitivity of detecting local vibrational modes (LVMs) even in highly absorbing spectral regions. This photoconductive technique allowed us to confirm a recent suggestion of a new multicenter bond for hydrogen in ZnO [A. Janotti and C. G. Van de Walle, Nature Mater. **6**, 44 (2007)]. The two LVMs of the hydrogen substituting oxygen in ZnO are identified at 742 and 792 cm$^{-1}$. The modes belong to a nondegenerated $A_1$ and a twofold degenerated $E$ representations of the $C_{3v}$ point group. The tetrahedral coordination of the hydrogen atom is the result of a newly detected multicenter bond for defects in solids.

DOI: 10.1103/PhysRevLett.108.165501 PACS numbers: 61.72.J−, 63.20.Pw, 71.55.Gs, 82.30.Rs

Local vibrational modes (LVMs) are ‘‘fingerprints’’ of light defects in solids which characterize the symmetry and chemistry of the defects in the host lattice and the type of interaction with the neighbors. LVM detection by Fourier-transformed IR absorption spectroscopy has been developed as the most versatile technique for defect studies [1]. The theoretical description of defects in solids has advanced lately and allows the calculation of LVMs to a very high precision. Hence, predictions of defect properties can be easily verified by LVM spectroscopy.

Recent first principles calculations by Janotti and Van de Walle suggested that hydrogen substituting for oxygen ($H_O$) in the binary metal oxides ZnO and MgO binds equally to all metal neighbors. The authors introduced the concept of the *hydrogen multicenter bond* in solids to visualize their results [2]. Theoretical considerations also indicate the general role of multicenter bonds for hydrogen transport, storage mechanisms and for the influence on magnetic properties [3–6].

Calculated LVMs of hydrogen substituting for oxygen in ZnO and MgO were found at 760(50) and 995(50) cm$^{-1}$, respectively [2]. These values are lower than the LVMs of 1497 and 1490 cm$^{-1}$ for two-center H-Zn and H-Mg bonds due to the higher coordination numbers and the larger H-metal-atom distances in the multicenter configurations [7]. Infrared absorption lines at 1027, 1034, and 1056 cm$^{-1}$ have been reported in MgO, whose frequencies match the theoretical predictions for the $H_O$ species [8,9].

The calculation by Janotti and Van de Walle was challenged by Takenaka and Singh [10] and more recently by Du and Singh [11] who, in the framework of standard local density approximation have found that hydrogen trapped in anion vacancies of Zn-based II-VI semiconductors is stabilized by the ionic bonding rather than by the multicenter covalent bond. In the case of ZnO, however, Du and Singh agree with Janotti and Van de Walle that hydrogen is fourfold coordinated giving rise to a local vibrational mode at 723 cm$^{-1}$.

Photoluminescence and photoconductivity studies unveiled the shallow donor behavior of $H_O$ in ZnO based on which it was concluded that it is hydrogen substituting for oxygen that is responsible for the unintentional *n*-type conductivity of ZnO grown by chemical vapor transport [12–14]. The chemical bonding of hydrogen in the oxygen vacancy was, however, not addressed in these experimental studies. The predicted LVM frequency of the complex is positioned in the strongly absorbing region of ZnO close to the Reststrahlen band [15], which made IR absorption and thus direct verification of the theoretical predictions practically impossible.

In this Letter we present experimental approach for the detection of the LVMs, which is suitable for probing vibrational modes even in highly absorbing regions of the spectrum. The results of a photoconductivity study of hydrogenated ZnO reveal the LVMs of $H_O$ and demonstrate that hydrogen substituting for oxygen in ZnO is equally bound to all four neighboring Zn atoms.

The nominally undoped ZnO samples used in this work were grown from the vapor phase at the Institute for Applied Physics, University of Erlangen, Germany [16,17]. The hexagonal prisms were cut into thin plates with typical dimensions of $10 \times 3 \times 0.3$ mm$^3$. Hydrogen or deuterium was introduced into the samples via thermal treatments in sealed quartz ampules, filled with $H_2$ or $D_2$ gas (pressure of 0.5 bar at room temperature). The treatments were performed at 730–800 °C within 1 h and were terminated by quenching to room temperature in water. To produce Ohmic contacts, the samples were first etched with orthophosphoric acid (85%) for 1 min at room temperature. Afterwards, two contacts with an area of approximately $2 \times 2$ mm$^2$ were generated by scratching an In-Ga eutectic onto the sample surface.

The photoconductivity measurements were performed with a Bomem DA3.01 Fourier spectrometer equipped with a globar light source and a KBr or Mylar (3.5 $\mu$m thick) beam splitter. The samples were positioned in an exchange-gas cryostat equipped with polypropylene or

ZnSe windows. The frequency range 100–5000 $\mathrm{cm}^{-1}$ could be covered. The spectral resolution was 1 to 4 $\mathrm{cm}^{-1}$. The temperature of the sample was stabilized within 0.4 K in the range of 10–14 K. Polarized light was produced by a wire-grid polarizer on a KRS-5 substrate in front of the cryostat.

Photoconductivity spectra of ZnO are recorded in two spectral regimes: A region below the Reststrahlen band revealing internal electronic transitions of shallow donors and a region above the Reststrahlen band, which shows the direct ionization of these donors into the conduction band. The upper spectrum of Fig. 1(a) was obtained from a ZnO sample treated in $H_2$ gas at 735 °C. Such a treatment results in the formation of $H_O$ close to the sample surface which gives rise to the internal $1s$-to-$2p$ donor transition at 265 $\mathrm{cm}^{-1}$ [12,18]. Furthermore a band at about 310 $\mathrm{cm}^{-1}$ can be seen, which consists mainly of the internal electronic transition from the ground $1s$ to the first excited $2p$ state of the Al and interstitial hydrogen ($H_{BC}$) shallow donors [12,19]. The upper part of Fig. 1(b) presents a spectrum of the hydrogenated sample which has been background subtracted using a photoconductivity spectrum of a sample where no $H_O$ was incorporated. Note that the features marked by an asterisk occur at the positions of strong two-phonon absorption bands of ZnO [15]. They are a result of a nonperfect background subtraction. However, independent of the subtraction procedure, two dips at 742 and 792 $\mathrm{cm}^{-1}$ are always seen in this spectrum, whose frequencies match the theoretical prediction for the LVMs of hydrogen substituting for oxygen in ZnO [2,11].

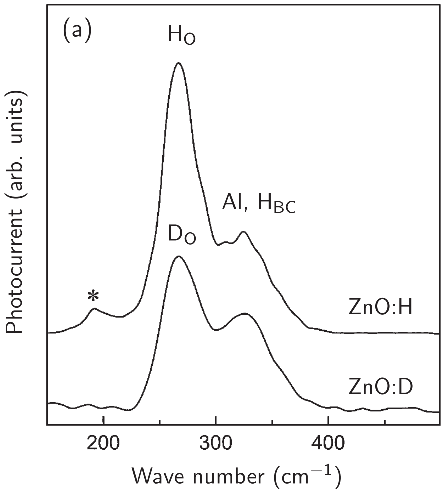

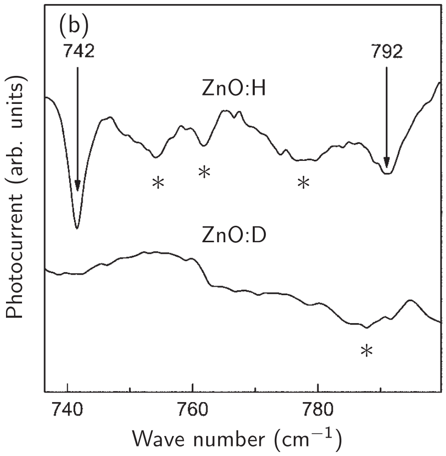

FIG. 1. Photoconductivity spectra of ZnO recorded at 11–12 K. The samples were treated in the $H_2$ or $D_2$ gas at 735 °C. (a) Internal transition of shallow donors. (b) Direct ionization of shallow donors. All spectra shifted vertically for clarity. In (b), the spectra are background corrected to a reference. The features marked by an * are not related to the defect discussed in this paper.

Frequencies of local vibrational modes are inversely proportional to the square root of the masses of vibrating species. This allows us to verify the nature of the 742 and 792 $\mathrm{cm}^{-1}$ lines since electronic transitions of $H_O$ practically do not change after replacement of hydrogen with deuterium [12]. The lower spectra in Fig. 1 were obtained from a sample treated in the $D_2$ gas. As expected, the $1s$-to-$2p$ transition of the $D_O$ donor does not shift and occurs at the same frequency of 265 $\mathrm{cm}^{-1}$. On the other hand, no absorption lines at 742 and 792 $\mathrm{cm}^{-1}$ are seen in the spectrum of the deuterium-treated ZnO which agrees with the assignment of these lines to the vibrational modes of hydrogen. Note that the expected local vibrational modes of $D_O$ at about $742/\sqrt{2} = 525$ and $792/\sqrt{2} = 560$ $\mathrm{cm}^{-1}$ are to be found within the Reststrahlen band of ZnO where practically no light can enter the sample [15], which explains why these LVMs can be detected neither by photoconductivity nor IR absorption.

Formation of $H_O$ in ZnO occurs via oxygen out-diffusion and subsequent trapping of interstitial hydrogen at the oxygen vacancies in the near surface layer. The thickness of this layer $d$ depends on the temperature and duration of the treatment [12,18]. With the parameters employed in our experiments (735 °C, 1 hr) it should result in $d \approx 2.5$ $\mu$m. This property was used to further corroborate the origin of the 742 and 792 $\mathrm{cm}^{-1}$ modes. In order to do this, photoconductivity measurements were performed after a series of etchings of a hydrogenated ZnO sample in orthophosphoric acid (for details of the etching procedure see Ref. [12]).

The spectrum in Fig. 2(a) was obtained directly after the hydrogen treatment. Both electronic transitions of $H_O$ at 265 $\mathrm{cm}^{-1}$ and the 742 $\mathrm{cm}^{-1}$ mode are seen. On the other hand, no $H_O$-related signals are detected in spectrum (b) recorded after removal of 3.5 $\mu$m from each surface of the sample. This is consistent with the known properties of hydrogen trapped in the oxygen vacancy in ZnO and supports the assignment of the 742 and 792 $\mathrm{cm}^{-1}$ modes to the LVMs of hydrogen trapped in the oxygen vacancy. Note that the concentration of the $H_O$ complex in this sample is much weaker compared to the one presented in Fig. 1.

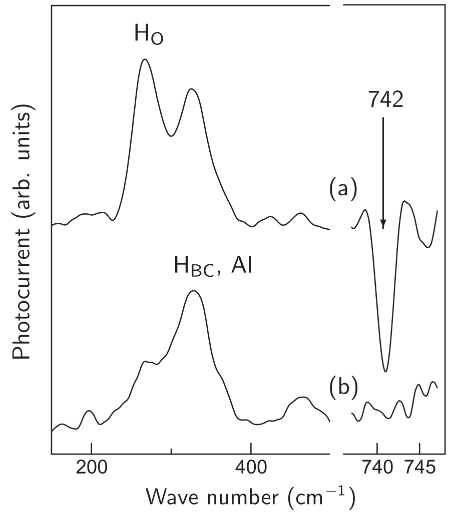

FIG. 2. Photoconductivity spectra obtained at 13 K from a ZnO sample thermally treated in the $H_2$ gas at 735 °C: (a) directly after the treatment and (b) after a removal of about 3.5 $\mu$m from each surface of the sample. The spectra were shifted vertically for clarity and background corrected to a reference.

Further insight into the nature of the 742 and 792 cm$^{-1}$ modes can be obtained from polarized photoconductivity measurements presented in Fig. 3. The 742 cm$^{-1}$ mode is polarized parallel, whereas the one at 792 cm$^{-1}$ perpendicular to the $c$ axis of the crystal. The frequencies of the modes $\sigma$ of $H_O$ can be obtained in the valence force approximation from the secular equation [20]

$$\|\boldsymbol{F}\boldsymbol{G} - \sigma^2\boldsymbol{E}\| = 0, \tag{1}$$

where $\boldsymbol{E}$ is the identity matrix and

$$\boldsymbol{G} = \begin{pmatrix} 1/\mu & \cos\varphi/m_H & \cos\varphi/m_H & \cos\varphi/m_H \\ \cos\varphi/m_H & 1/\mu & \cos\varphi/m_H & \cos\varphi/m_H \\ \cos\varphi/m_H & \cos\varphi/m_H & 1/\mu & \cos\varphi/m_H \\ \cos\varphi/m_H & \cos\varphi/m_H & \cos\varphi/m_H & 1/\mu \end{pmatrix},$$

$$\boldsymbol{F} = \begin{pmatrix} f_\parallel & 0 & 0 & 0 \\ 0 & f_\perp & 0 & 0 \\ 0 & 0 & f_\perp & 0 \\ 0 & 0 & 0 & f_\perp \end{pmatrix}. \tag{2}$$

Here, $1/\mu = 1/m_{Zn} + 1/m_H$ with $m_{Zn} = 65$ a.u.; $f_\parallel$ and $f_\perp$ are the force constant parallel and perpendicular to the $c$ axis, respectively; and $\varphi = 109°47'$ is the $\sphericalangle$ Zn-H-Zn angle, which we for simplicity assumed to be tetragonal.

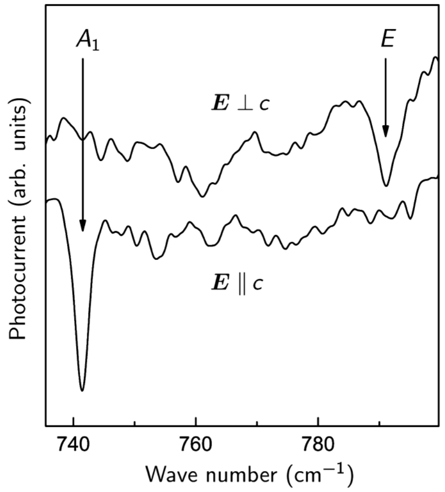

FIG. 3. Photoconductivity spectra taken at 13 K from a hydrogenated ZnO sample background corrected with a reference sample without $H_O$. The incident light was polarized perpendicular (top) and parallel (bottom) to the $c$ axis, respectively.

The results of the fit presented in Table I suggest that the 742 cm$^{-1}$ mode should be associated with the nondegenerate mode $A_1$, whereas the one at 792 cm$^{-1}$ transforms as the double degenerate mode $E$ of the $C_{3v}$ point group. The mode at 83 cm$^{-1}$ basically does not involve the motion of hydrogen and falls beyond the detection limit of our setup at 100 cm$^{-1}$.

These results can be interpreted on the basis of the universal empirical relation between the interatomic distance $l$ and the vibrational frequencies $\sigma$ of diatomic molecules obtained by Morse [21]

$$l^3\sigma = \text{const.} \tag{3}$$

From the known parameters of the ZnH molecule ($l = 1.595$ Å, $\sigma = 1497$ cm$^{-1}$ [7]) and the weighted average frequency of $H_O$ ($775 = (742 + 2 \times 792)/3$ cm$^{-1}$) we obtain that the mean distance between hydrogen and the neighboring Zn atoms in the defect equals 1.99 Å. This is very close to the average Zn-O bond length in ZnO and agrees with the theoretical value reported by Du and Singh [11].

Furthermore, Eq. (3) can be employed to estimate the difference between the Zn-H bond lengths parallel $l^{\parallel}_{\text{Zn-H}}$ and perpendicular $l^{\perp}_{\text{Zn-H}}$ to the $c$ axis. With the values of $f_\parallel$ and $f_\perp$ (see Table I) we find that $l^{\parallel}_{\text{Zn-H}}$ is 3% longer than $l^{\perp}_{\text{Zn-H}}$. Here, we took into account that $\sigma \propto \sqrt{f}$. This correlates with the parameters of the perfect ZnO lattice with $l^{\parallel}_{\text{Zn-O}} = 1.986$ Å and $l^{\perp}_{\text{Zn-O}} = 1.952$ Å, yielding $\Delta l/l = 2\%$ [22].

TABLE I. Best-fit parameters of Eq. (2) for the LVMs of $H_O$.

| Mode | $\sigma$ (cm$^{-1}$) | Polarization |
|---|---|---|
| $A_1$ | 83 | $\parallel c$ |
| $A_1$ | 742 | $\parallel c$ |
| $E$ | 792 | $\perp c$ |
| $f_\parallel = 0.585$ N/m | | $f_\perp = 0.699$ N/m |

Finally, we comment on the charge state of $H_O$. Obviously, only the neutral donor can give rise to the 742- and 792-$cm^{-1}$ dips in the photoconductivity spectra. As a shallow impurity, however, $H_O$ is ionized at room temperature, which should affect the frequencies of the LVMs. The wave function of an electron is weakly localized at the core of a shallow donor which leads us to the suggestion that the LVMs of $H_O^+$ are close to those of the neutral defect (see, for example, Ref. [23]).

In conclusion, a sensitive photoconductive technique for probing local vibrational modes in highly absorbing regions of the spectrum is explored to investigate LVMs of hydrogen substituting for oxygen in ZnO. Our study reveals that in the neutral charge state, the defect has LVMs at 742 and 792 $cm^{-1}$, which are assigned to the $A_1$ and $E$ representations of the $C_{3v}$ point group, respectively. These results agree with the theoretically predicted properties of the fourfold coordinated hydrogen trapped in the oxygen vacancy.

This work was supported by the Deutsche Forschungsgemeinschaft (Grant No. LA 1397/4-1).

---

*edward.lavrov@physik.tu-dresden.de

[1] *Identification of Defects in Semiconductors*, edited by M. Stavola Semiconductors and Semimetals (Academic Press, San Diego, 1999), Vol. 51B.

[2] A. Janotti and C. G. Van de Walle, Nature Mater. **6**, 44 (2007).

[3] P. Tarakeshwar, T. J. D. Kumar, and N. Balakrishnan, J. Chem. Phys. **130**, 114301 (2009).

[4] D. Stradi, F. Illas, and S. T. Bromley, Phys. Rev. Lett. **105**, 045901 (2010).

[5] M. Assadi, Y. Zhang, and S. Li, J. Phys. Condens. Matter **22**, 156001 (2010).

[6] T. A. Abtew, B. Shih, P. Dev, V. H. Crespi, and P. Zhang, Phys. Rev. B **83**, 094108 (2011).

[7] *CRC Handbook of Chemistry and Physics*, edited by D. R. Lide (CRC Press LLC, Boca Raton, 2001), 82nd ed.

[8] R. González, Y. Chen, and M. Mostoller, Phys. Rev. B **24**, 6862 (1981).

[9] V. M. Orera and Y. Chen, Phys. Rev. B **36**, 6120 (1987).

[10] H. Takenaka and D. J. Singh, Phys. Rev. B **75**, 241102(R) (2007).

[11] M.-H. Du and D. J. Singh, Phys. Rev. B **79**, 205201 (2009).

[12] E. V. Lavrov, F. Herklotz, and J. Weber, Phys. Rev. B **79**, 165210 (2009).

[13] B. K. Meyer, H. Alves, D. M. Hofmann, W. Kriegseis, D. Forster, F. Bertram, J. Christen, A. Hoffmann, M. Straßburg, M. Dworzak *et al.*, Phys. Status Solidi B **241**, 231 (2004).

[14] A. Schildknecht, R. Sauer, and K. Thonke, Physica (Amsterdam) **340–342B**, 205 (2003).

[15] E. V. Lavrov, F. Börrnert, and J. Weber, Phys. Rev. B **72**, 085212 (2005).

[16] G. Müller and R. Helbig, J. Phys. Chem. Solids **32**, 1971 (1971).

[17] R. Helbig, J. Cryst. Growth **15**, 25 (1972).

[18] F. Herklotz, E. Lavrov, and J. Weber, Physica B (Amsterdam) **404**, 4349 (2009).

[19] F. Herklotz, E. V. Lavrov, J. Weber, G. V. Mamin, Y. S. Kutin, M. A. Volodin, and S. B. Orlinskii, Phys. Status Solidi B **248**, 1532 (2011).

[20] E. B. Wilson, J. C. Decius, and P. C. Cross, *Molecular Vibrations* (Dover, New York, 1980).

[21] P. M. Morse, Phys. Rev. **34**, 57 (1929).

[22] H. Karzel, W. Potzel, M. Köfferlein, W. Schiessl, M. Steiner, U. Hiller, G. Kalvius, D. Mitchell, T. Das, P. Blaha *et al.*, Phys. Rev. B **53**, 11 425 (1996).

[23] F. Herklotz, E. V. Lavrov, and J. Weber, Phys. Rev. B **83**, 235202 (2011).